Identification of Novel MiR-122 Targets with Potential Role in Hepatocellular Cancer

Research Thesis

Presented in partial fulfillment of the requirement for graduation *with research distinction* in the undergraduate colleges of The Ohio State University.

By

Chelsey Williams

The Ohio State University
April 2016

Project Advisor: Dr. Kalpana Ghoshal, College of Medicine, Dept. of Pathology

Table of Contents

I. Abstract

MicroRNA 122 (MiR-122) is an abundant liver-specific miRNA which serves to regulate hepatic metabolism, and functions as a tumor suppressor. We are determining how a tiny, twenty-two nucleotide microRNA maintains homeostatic liver function. Loss of hepatic phenotype, metastasis, and poor prognosis are characteristics of down regulation of miR-122 expression. Spontaneous Hepatocellular Carcinoma (HCC) development has been observed in liver-specific (LKO) and germ-line (KO) knockout miR-122 mice. Results of Ago-HITS-CLIP analysis conducted in livers of 6 week-old wild type and KO mice confirmed ~1800 miR-122 binding sites present in wild-type, but absent in KO livers. MiR-122 binding sites were identified on the 3' untranslated regions (3'-UTR) of the snail family zinc finger 2 (Snai2) gene, TIMP metallopeptidase inhibitor 2 (Timp2) gene, LIM domain kinase 1 (Limk1) gene, Hepatocyte Nuclear Factor 4 alpha (Hnf4a) and Pygopus Family PHD Finger 2 (Pygo2).

The encoded protein of Snai2 is involved in epithelial mesenchymal transitions, and has the ability to enable the cell to resist apoptotic signals. Timp2 functions as a metastasis suppressor. Limk1 regulates actin polymerization through phosphorylation and subsequent inactivation of cofilin, while Hnf4a regulates liver development. Pygo2 is involved in signal transduction of the Wnt and GPCR pathways. The presence of these discovered binding sites highly suggests targeting and regulation by miR-122. These genes are potentially involved in liver pathogenesis, and could be crucial with respect to determining HCC progression. To explore the possibility of targeting and regulation by miR-122, real-time reverse-transcription polymerase chain reaction (qRT-PCR) was conducted. We hypothesized that in the absence of miR-122, expression levels of these genes would be increased. These five targets were found to be highly expressed in miR-122 knockout mice. RNA-sequencing analysis suggests that these

genes are undergoing regulation by miR-122. Snai2 has been validated as a direct miR-122 target using luciferase assay technology with hepatoma (Hepa) cells. Snai2 has been further validated using site-directed mutagenesis in Hepa cells. Broader implications of this study include miR-122 itself or Snai2 being targeted for HCC therapy in human patients.

II. Background

MicroRNAs (miRNAs) are short, noncoding RNAs composed of approximately 22 nucleotides that serve to negatively regulate protein-coding genes [1]. Following their transcription into hairpin pri-microRNAs in the nucleus, they are then cleaved to their pre-microRNA forms. Exportin proteins in combination with RAN-GTP allow for RNA nuclear export into the cytoplasm, where the pre-microRNA is again cleaved by Dicer, and the 5' strand is uploaded to the RNA-induced silencing complex (RISC) in conjunction with Argonaute 2 proteins [1]. After undergoing processing in the RISC complex, the microRNA is now mature and ready to conduct its cellular functions, such as mRNA target cleavage, translational repression and/or mRNA adenylation (Figure 1).

In liver development, miRNAs are known to be important in cell differentiation as well as organ development [1]. MicroRNA-122 (miR-122) is essential for maintenance of liver homeostasis, and is conserved across vertebrate species [2,3,4]. Its complete conservation reflects its critical role in the liver. As the most abundant liver-specific miRNA, it accounts for 70% of total liver microRNA as demonstrated when cloning varying mouse tissue miRNA. MiR-122 serves to regulate a variety of diverse functions. These include glucose homeostasis, lipid metabolism, and cholesterol [2,3]. It has also been shown to promote hepatitis C virus (HCV) replication [2]. Its inhibition results in dysregulation of hepatic lipid metabolism and iron homeostasis [4]. While miR-122 is not necessary for embryogenesis in mice (as demonstrated by

successful generation of germ-line knockout mice), complete loss of miR-122 results in spontaneous steatohepatitis early in life and hepatocellular carcinoma (HCC) with age [3,4]. Additionally, studies show that ectopic expression of miR-122 in both human and mouse stem cells results in differentiation into hepatocyte-like cells in vitro. This suggests that depletion of miR-122 levels in humans may also have severely negative consequences in humans [3]. Loss of miR-122 also results in upregulation of its target genes, while its overexpression in HCC cell lines reduces tumerigenesis [2]. Ultimately, miR-122's roles as a tumor suppressor and master regulator of other protein-coding genes, along with its specificity to the liver makes it an attractive target for gene therapy, both as a mimic and anti-miRNA. It also serves as a key prognostic marker in identifying patients with advanced hepatocellular carcinoma (HCC) [4].

Located on chromosome 18, miR-122 is first transcribed as an approximately 7.5 kilonucleotide primary transcript from an intergenic region [2]. It is then processed to a 66 nucleotide precursor RNA, which is then spliced to a tiny, 22 nucleotide mature miR-122. It is stabilized by the addition of a single adenosine to it's 3' –end by GLD2, a noncanonical cytoplasmic poly(A) polymerase. This stabilization is thought to be the cause of miR-122 abundance [4]. Mature miR-122 interacts with its target mRNAs through binding at a variety of seed sites, located on its 3'UTR (Figure 2).

HCC is the most common occurring liver cancer, and is the fifth most prevalent cancer in the world [2]. It serves as the third leading cause of cancer related deaths, and its incidence has nearly tripled in the United States over the past 20 years [5]. HCC often arises in patients experiencing chronic liver disease, cirrhosis, and inflammation. Both alcoholic and non-alcoholic fatty liver disease promote HCC development. Other primary risk factors for HCC include hepatitis B and C virus infections, as well as genetic mutations [4]. Reduced miR-122 expression

is associated with spontaneous development of HCC, and correlates with poor prognosis and metastasis in human HCC patients [6]. Few therapies exist to treat HCC, and since early diagnosis of HCC is difficult to achieve, HCC mortality rates continue to steadily rise [4]. The disease is so progressive that death usually occurs within 10 months of initial diagnosis [7]. Therefore, investigation of specific genetic alterations is vital to the pursuit of novel HCC therapies.

Gene therapy has been utilized to treat human patients with HCC to restore homeostatic liver function and normal gene expression. While siRNA-mediated silencing of a disease-causing target gene serves as a potential option, it is likely that redundant genes possessing complementary functions could compensate the function of a knockdown gene. Many studies relating microRNAs to a specific disease are centered on identifying and validating candidate target genes as predicted by different databases [3]. This is a necessary step prior to evaluating the biological functions of target genes and eventual development of gene-specific therapies for clinical trials.

The snail family zinc finger 2 (Snai2) gene encodes for a zinc finger transcription factor that represses transcription through binding to E-box consensus elements. Snai2 can activate its own expression through binding to E-box elements in the binding regions of its own promoter [8,9]. Structurally, it possesses five zinc fingers in its C-terminal domain which interact with the canonical E box sequence [9,10,11]. It has previously been found to be overexpressed in many cancers, including lung, esophageal, colorectal, gastric, pancreatic, breast, prostate, ovarian, leukemia, and glioma. Its overexpression is described as a hallmark of epithelial mesenchymal transition (EMT), and low survival [10,11]. EMT occurs during adult wound healing as well as

cancer metastases [10]. The process involves a decrease in expression of cell junction components, resulting in a motile and invasive mesenchymal phenotype.

Timp2 was recently discovered to be the most significantly downregulated member of the TIMP gene family in human HCCs. Additionally, it was found that stable silencing of Timp2 in HCC cell lines enhanced cell invasiveness. In xenograft mouse models, it was demonstrated that ectopic expression of Timp2 in the HCC cell line MHCC-97L significantly reduced HCC progression and metastasis [12]. Findings from this same paper further established that Timp2 is an important regulator of extracellular matrix degradation [12]. These newfound discoveries are indicative that Timp2 is heavily involved with HCC progression.

Increased expression levels of LIMK1 are correlated with tumor differentiation, cell invasiveness, cell motility, and poor patient prognosis [13,14]. As a serine/threonine protein kinase, it plays a crucial role in regulating dynamics of actin filaments. LIMK1 inhibitors have additionally been used to block tumor cell proliferation by disrupting mitotic microtubule organization in kidney cancer cells [15]. Hnf4a regulates epithelial cell function, and functions as a nuclear transcription factor [17]. Pygo2 functions in the high-conserved Wnt/B-catenin signaling pathway, and has additionally served as a prognostic marker for glioma [18].

III. Materials and Methods

1. HITS-CLIP

High-Throughput sequencing with cross-linking and immunoprecipitation with the Argonaut protein complex(Ago-HITS-CLIP) was used to determine sites on mRNAs believed to be miR-122 targets. This technique was originally developed as a means of further understanding how protein-RNA complexes interaction regulate gene expression in living cells [19,20]. Ago-HITS-CLIP allows for a genome-wide screen of RNA binding sites in vivo. Following UV irradiation of mouse liver samples, the cells underwent lysis, partial RNase digest, and immunoprecipitation (Figure 3).

Argonaute proteins bind different classes of small, non-coding RNAs. By measuring argonaute pull-down of miR-122 specific seed sites, Ago-HITS-CLIP thus also measures the binding of miR-122 to target genes containing the miR-122 binding site. MiR-122 binding is visualized in the form of peaks on a graph (Figure 4). In wild-type mice, pull-down of genes with the specific miR-122 binding sites will occur. This is because miR-122 is present in these mice, and thus can bind to its respective target genes. Ago-HITS-CLIP data will register a peak at those regions.

In miR-122 KO mice, there will be significantly less or complete lack of pull down of miR-122 sequence-specific gene regions by the Argonaute protein complex. This is because miR-122 is absent from these mice, and thus cannot bind to its complementary sites of target genes. This will cause the peaks shown on HITS-CLIP data to disappear

The differences in occurring peaks shown on HITS-CLIP data from wild-type and KO mice were used to determine the likelihood of miR-122 regulation. Additionally, we ensured the

peak region contained the miR-122 seed site (CACTCC) and confirmed that the Snai2 region was conserved in humans (Figure 5). The miR-122 binding site appears as a 7A1mer in mice and as a 6mer in humans (refer to figure 2 for specific seed sequences).

2. RNA-Sequencing

RNA-sequencing (RNA-seq) was used to measure relative gene expression of wild-type mice versus miR-122 KO mice. This assay measures the number of mRNA reads for a multitude of genes, both known and unknown, in wild-type and KO mice. We are particularly interested in the predicted target genes of miR-122. This assay served as a validation strategy to determine the mRNA level of miR-122 targets and in-vivo function of miR-122. The relative gene expression was calculated by taking the log of the ratio of wild-type mRNA reads/KO mRNA reads (Table 1). It was predicted that KO mice would contain more mRNA reads of suspected target genes because miR-122 was not present to regulate those genes. Thus, it was also thought that prospective targets of miR-122 would have WT/KO mRNA read ratios of less than 1. The logs of these values would then be negative, indicative of relative fold change.

A comparison of RNA-seq data and Ago-HITS-CLIP data results in an inverse relationship in terms of the peaks which register on the raw data. MiR-122 target genes in RNA-seq will demonstrate a peak, while miR-122 target genes defined by Ago-HITS-CLIP will not register a peak (Figure 6). This peak comparison between the two data set is what allowed us to identify particular targets.

3. qRT-PCR analysis of miR-122 targets in liver RNA isolated from the wild type and KO Mouse cDNA

Mouse RNA was extracted from miR-122 KO mice using TRIZol (Life Technologies, Inc). 2 ug of RNA was converted to cDNA (Bioline). The reaction was conducted at 25°C for 10 minutes, 37°C for 2 hours, and 85°C for 5 minutes. Samples were treated with with DNaseI to remove residual DNA copurified with RNA. SYBR Green fluorescent dye, 3'UTR Snai2 specific primers, and the newly-made cDNA was then utilized in qRT-PCR. Housekeeping gene GAPDH (involved in catalyzing glucose breakdown) was used as a normalizer.

4. 3'UTR Amplification, Isolation, and Purification

Polymerase Chain Reaction was conducted with Accuprime Polymerase and dNTPs to amplify the 3'UTR regions of mouse Snail2, Timp2, and Hnf4a. The PCR was run for 27 cycles of 30 sec at 94°C, 30 seconds at 56°C, and 30 seconds at 68°C. DNA loading buffer 6X was added to the PCR product and the DNA was run on a 1.5% agarose gel (1.5g agarose/ 100 mL 1X Tris-Acetate EDTA Buffer) containing ethidium bromide at 80 V for 45 minutes. The PCR product was run alongside a 100 bp ladder to ensure the product was the correct size. The band was then visualized with ultraviolet light, and cut from the gel with a razor. Remaining agarose along with other impurities were removed from the PCR product using QIAquick Gel Extraction Kit according to the manufacturer's instructions. Approximately 450 ng of product was digested overnight at 37°C with restriction enzymes Not I and Xho I. 50 ng of psiCHECK2 was simultaneously digested under the same conditions in preparation for ligation of the 3'UTR sequence into

the psiCHECK2 vector. The 3'UTR PCR product was purified using Qiagen PCR Purification Kit following the manufacturers instructions.

a. Vector Ligation

50 ng of psiCHECK2 (Figure 7) were combined with approximately 10 ng of the digested 3'UTR gene insert. 1 uL of 10X QuickLigase and 5 uL of 2X Ligase Buffer were added to the reaction, and the reaction was incubated at 25°C for 30 minutes.

b. Transformation

Clones were amplified by transforming the newly-ligated constructs into competent DH5α cells. DH5α cells were thawed on ice for 15 minutes. 25 uL of cells were combined with 10uL of freshly ligated plasmid. The plasmid was added to the cells to reduce cellular damage. The mixture was chilled on ice for 30 minutes prior to undergoing a heat shock at 37°C for 2 minutes. The mixture of cells and plasmid was then chilled on ice for 5 minutes. After addition of 0.5 mL of pure Luria-Bertani broth (LB), the cells were rocked at 37°C and 75 rpm for 1 hour. Cells were pelleted via centrifuge (5k rpm), and resuspended in 100 uL of media. The cell solution was spread on a sterile LB plate containing ampicillin. Bacterial colonies were grown for 16 hours at 37°C. Individual colonies were tested by PCR to identify positive clones (harboring specific 3'UTRs), allowed to grow in LB- ampicillin medium and plasmid DNAs of the cultures was purified using QIAprep Miniprep Kit. The recombinant psiCHECK2 DNAs were screened by digesting with Xho I and Not I followed by gel electrophoresis. Sanger

Sequencing confirmed that the vector contained the Snai2 sequence with the miR-122 binding site.

4. Transfection with psiCHECK2 Snai2

Transfection was conducted in the following manner with additional genes of Hnf4a and Timp2.

Mouse Hepa cells were seeded into 16 wells of a 24-well-plate (1.2 million cells/well). Next day, cells were transfected with 100 ng of the psicheck2-Snai2 vector in both the presence of 5 uM of miR-122 mimic as well as 5 uM of NC RNA (scrambled RNA). Additional Hepa cells were transfected simultaneously with 200 ng of psicheck2 to act as a control both the presence of 5 uM of miR-122 mimic as well as 5 uM of NC RNA (Figure 8). The transfection was performed in Minimum Essential Media (MEM) (Eagle) containing 10% (55 mL) Fetal Bovine Serum, 1.0% sodium pyruvate, 1.0% nonessential amino acids, and 1.0% Penicillin Streptomycin (for prevention of bacterial infection). Lipofectamine 3000 and p3000 (Invitrogen) reagents with optiMEM media (ThermoFisher Scientific) were utilized in the transfection according to the manufacturer's protocol. The Lipofectamine serves to form lipid complexes around the cloned vectors containing the gene of interest, and thus allows the vector to penetrate the double-layered lipid bilayer of the cell membrane. The reaction took place over a period of 6 hours at 37°C. Following the reaction, media was replaced with 600 uL of MEM. Cells were incubated for approximately an additional 24 hours at 37°C. Cells were washed twice with Phosphate-buffered saline (PBS) before lysis. Cell contents were transferred to individual Eppendorf tubes for further use in luciferase assay.

5. Luciferase Assay

Cell lysate was centrifuged for 5 minutes at 13200 RPM to pellet cell debris. MicroWin2000 machine was prepared via a washing with distilled water, and primed with luciferase assay reagents StopNGlo and Lar2. 10 uL of each cell lysate sample was loaded into a well of an opaque 96-well-plate. Analysis of the data was conducted by comparing differences between Snai2 transfected cells in the presence of miR-122 mimic versus in the presence of scrambled RNA negative control.

6. Site-Directed Mutagenesis

New 3' UTR primers were generated to mutate miR-122 binding site in the 3'-UTR of Snai2 using MacVector following published protocol [2]. The new primer sequences contain mutated base pairs relative to the primer sequences utilized in generating the original Snai2-psicheck2 vector (Table 2). 3'UTR amplification was performed in three steps with the new primers using Accuprime polymerase (Invitrogen) and dNTPs. The first PCR amplification step involved utilizing the forward site-directed mutagenesis primer with the original reverse 3'UTR primer. PCR was performed again using the original forward primer and the site-directed mutagenesis reverse primer. The PCR products from these two reactions were combined, and amplified using both the forward and reverse original primers to obtain the desired product containing a mutated miR-122 binding site. Plasmid isolation and purification, along with Transformation, Transfection, and Luciferase Reporter Assay were performed in the same fashion as with the original Snai2-psicheck2 vector.

IV. Results

Ago-HITS-CLIP and RNA-seq analysis indicated that Snai2, Limk1, Hnf4a, Pygo2, and Timp2 are targets of miR-122 (Table 1). A standard 2-tailed t-test was used to assess both qRT-PCR and Luciferase Reporter Assay data. A p-value of less than 0.05 was used to determine if the data gathered was significant. Real-time RT-PCR also indicated that these five genes were targets of miR-122 (Figures 9-12). Luciferase Reporter Assay analysis indicated that Snai2 is a direct target of miR-122, and site-directed mutagenesis confirmed Snai2 as a miR-122 target (Figures 13 and 14). Luciferase Reporter Assay analysis of Hnf4a and Timp2 produced negative data ($p > 0.05$) that could not confirm that these genes are miR-122 targets (Figures 15 and 16). This could be due to miR-122 having a higher binding affinity in vivo than when miR-122 target genes are associated with its own coding sequence instead of ligated to transgenes such as Luciferase. Also compared to 8mer and 7 mer miR-122 binding sites, 6mer binding sites have lower affinity that may not be strong enough to reduce luciferase expression. For future potential miR-122 targets, I would plan to investigate target genes of miR-122 as predicted by Ago-HITS-CLIP and RNA-seq that contained miR-122 8 or 7mer binding sites on their 3'UTRs.

V. Discussion and Final Conclusions

Before I contributed to the primary research goals in Dr. Ghoshal's laboratory, many potential miR-122 targets were still being investigated. Several genes had neither been confirmed or unconfirmed as direct targets, and little was known about the relationship between Snai2 and miR-122. Over time in the lab, I have greatly contributed to our laboratory's larger goal of determining miR-122 canonical pathways through extensive genotyping of mice to identify WT and KO mice, those were used for Ago-HiTS-CLIP analysis. I confirmed that Snail2 is a direct

target of miR-122. Because of my efforts, more is known about what genes are and are not targeted by master regulator miR-122 in liver carcinoma.

This research has extensive future implications. Gene therapy for cancer patients in becoming a more commonplace and effective method of treating cancer. Currently with only one available FDA-approved therapy for advanced stages of HCC, there is a clinical need for further treatment options. The current available therapy, sorafenib, is a multikinase inhibitor. While this treatment does provide minimal survival benefit for advanced HCC patients, the side effects are severe. A 2009 study produced data that did not support the use of sorafenib in patients. In our lab, it was previously demonstrated that miR-122 sensitizes HCC cells to sorafenib and that the cells have reduced malignant properties [7]. Previously in our lab it was demonstrated that delivery of the miR-122 minigene to mice containing a tetracyclin-repressible *MYC* transgene using a self-complementary adenoassociated virus (scAAV) resulted in dramatic inhibition of liver tumor growth [2] (Figure 17). Potentially in the future, therapeutic drugs could be developed to correct either low miR-122 expression levels, that may inhibit Snai2 to block EMT and metastasis. Transcription factors, in general, are not targetable using small molecule inhibitors. Thus, HCC expressing high levels of Snai2 could potentially be treated with miR-122. As a transcription factor, Snai2 is thought to possess several direct targets itself, such as transmembrane adhesion molecule E-cadherin [10]. Since this E-cadherin is a vital molecule in cell-cell adhesion and has already been shown on several occasions to increase proliferation and metastasis, its deregulation in conjunction with Snai2's deregulation by miR-122 poses an interesting path in examining Snai2's targets, along with its direct role in EMT and liver carcinogenesis.

VI. Figures and Tables

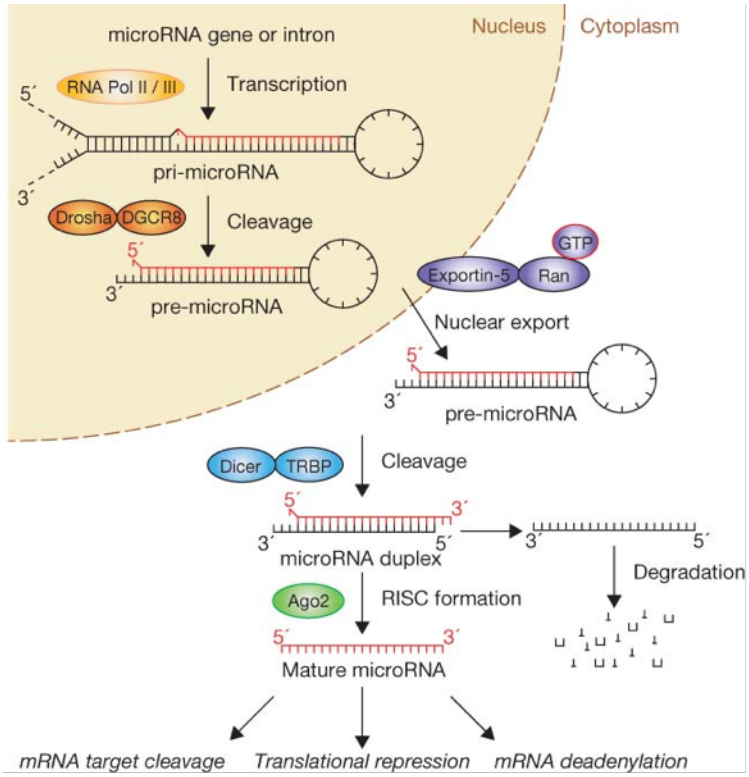

Figure 1: Standard microRNA processing mechanism.
Winter et al, Nature. 2009

Rank	Number of sites	MEME E-value	Sequence logo	miR-122 seed type
1	766	$8.5e^{-47}$		7merA1
2	494	$8.0e^{-44}$		8mer
3	583	$1.9e^{-37}$		G-bulged
4	520	$2.7e^{-23}$		7merM8
5	955	$9.0e^{-20}$		6mer

Figure 2: MiR-122 binding sites located on 3'UTR's of target genes were identified using HITS-CLIP. MiR-122 regulates its targets through interactions at these nucleotide sequences.

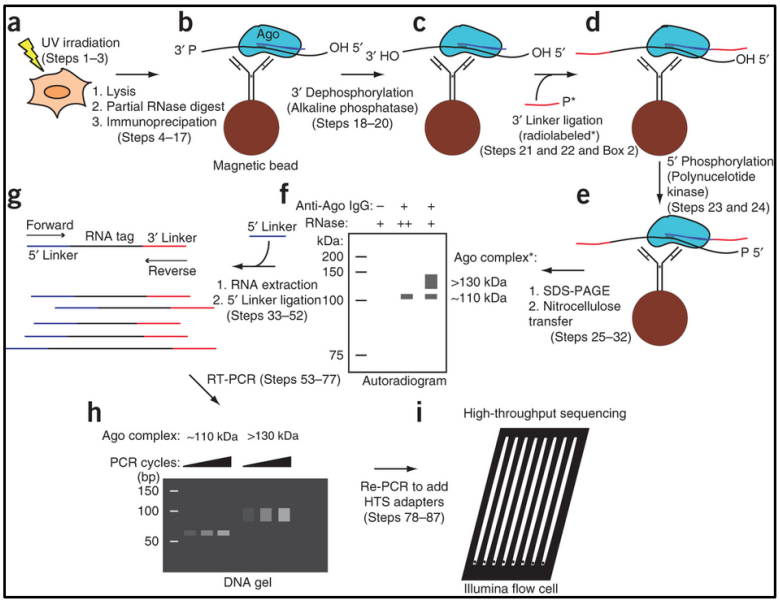

Figure 3: Ago-HITS-CLIP mechanism for detecting in-vivo microRNA binding

Moore MJ et al, Nature Protocols. 2014

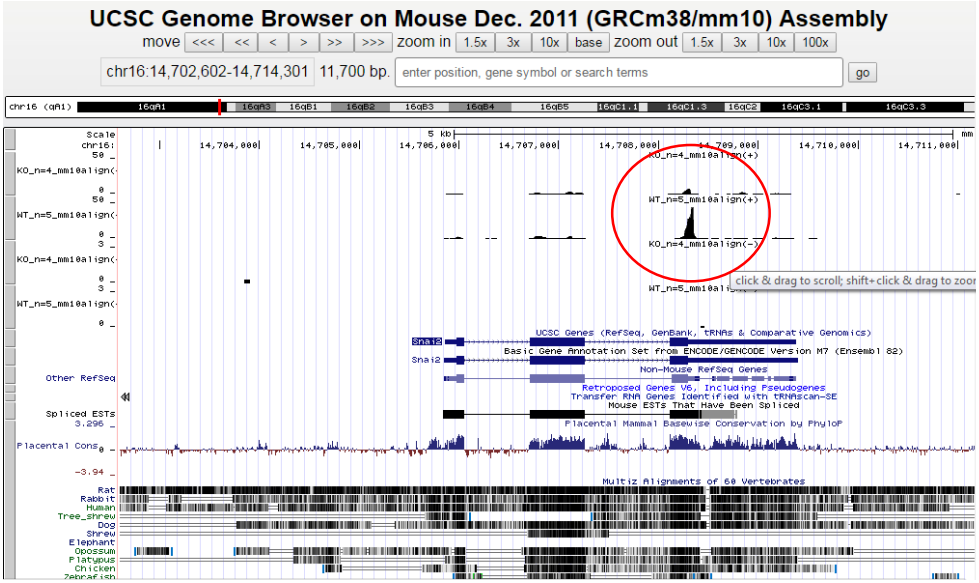

Figure 4: Ago-HITS-CLIP data shows peak present in location specific to miR-122. More pull-down of miR-122 target gene sequences by the Argonaut protein will lead to occurring peaks in miR-122 KO mice.

Figure 5: HITS-CLIP data shows peak present in location specific to miR-122

Gene Name	Seed Type (3'UTR)	Chromosome Location	RNA-Seq Values [Log_{10}(WT/KO)]
LIMK1	6mer	chr5	-1.290490681
TIMP2	6mer	chr11	-1.030708109
SNAI2	7A1mer	chr16	-0.487221716
Pygo2	6mer	chr3	-0.32605623
HNF4a	7A1mer	chr2	0.139545369

Table 1: Predicted MiR-122 target genes and RNA-Seq data. The more negative RNA-seq values indicate higher number of mRNA target gene reads in miR-122 KO mice.

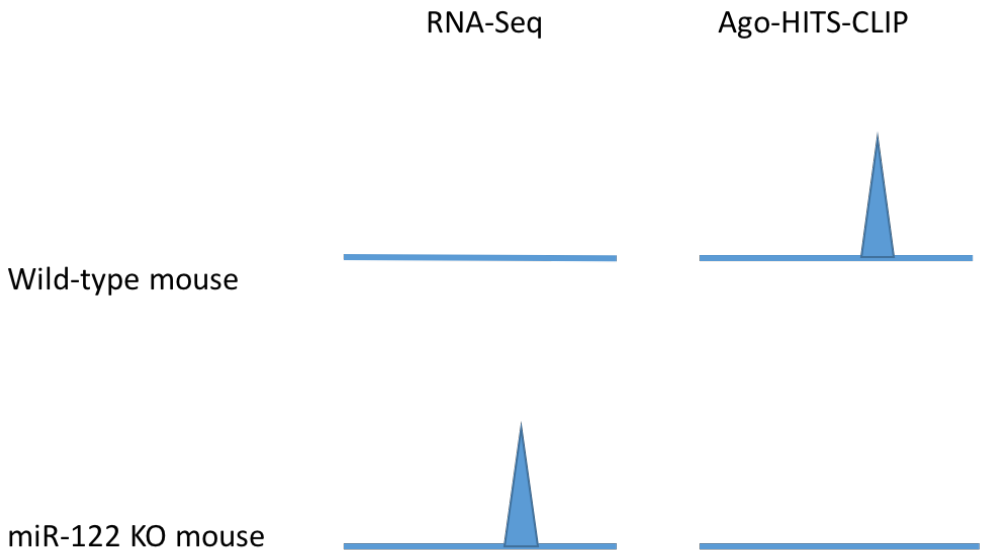

Figure 6: A comparison of wild-type and miR-122 KO mouse visual analysis of RNA-seq and Ago-HIT-CLIP data. In Ago-HITS-CLIP, the amount of miR-122 sequence-specific pull down is measured. A peak is shown at these sites in wild-type mice because miR-122 is present to actively bind to its seed sites located on the 3'UTRs of target genes. In RNA-Seq, mRNA levels are measured. In miR-122 KO mice, there is no miR-122 present to bind to its target sites and repress those genes. Thus the amount of mRNA reads for miR-122 target genes will be increased, gene expression will be upregulated, and a peak will register at those sites. This inversely correlated relationship between peaks is used as a confirmation strategy of miR-122 targets.

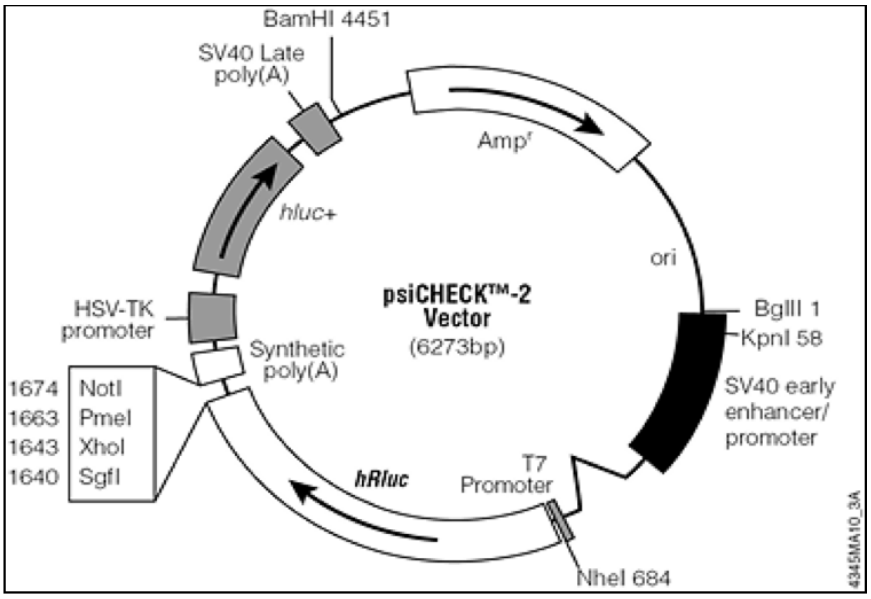

Figure 7: The 3'UTRs of miR-122 target genes were cloned into the psiCHECK2 vector using restriction enzymes Not1 and Xho1

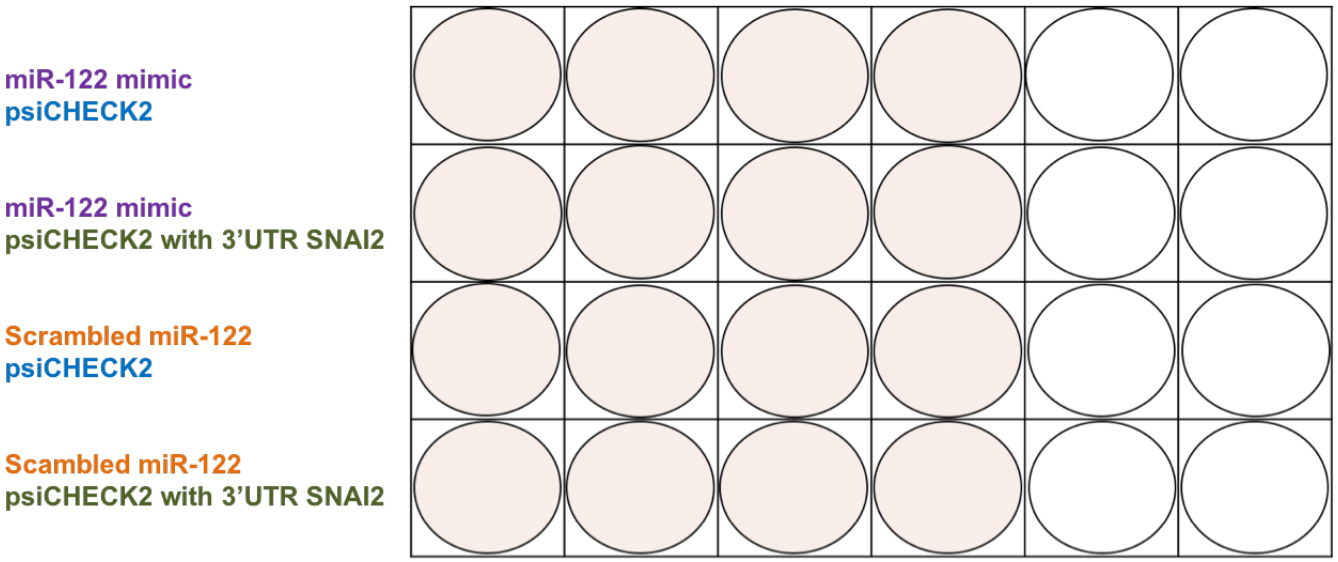

Figure 8: 24-well plate design for hepatocyte cell transfection with psiCHECK2 plasmid containing 3'UTR of gene of interest

SNAI2 Primers for 3'UTR Cloning and Site-Directed Mutagenesis		
	Forward Primer	Reverse Primer
3'UTR Cloning	5' CCG CTC GAG AAA AAC TGC TCC AAA ACC TT 3'	5' ATA AGA ATG CGG CCG CAC TAT TTG GTT GGT AAG CAC 3'
Site-Directed Mutagenesis	5' TGC ATT TCT TGT GAG GAA TGA CAA ATG A 3'	5' ATT TGT CAT TCC TCA CAA GAA ATG C 3'

Table 2: Primer sequences for 3'UTR cloning and site-directed mutagenesis

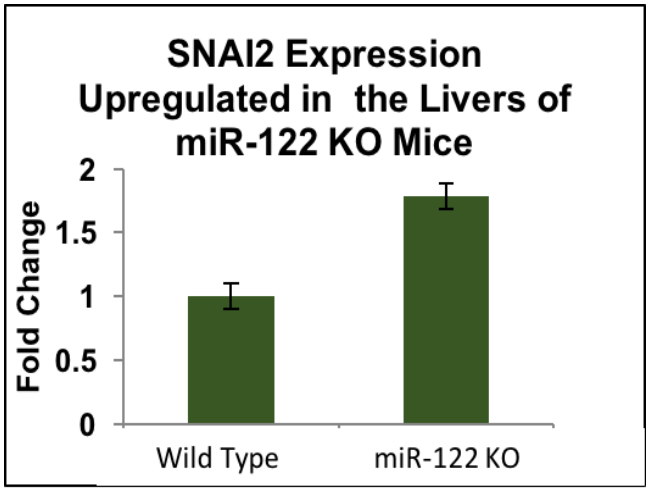

Figure 9: Real-time PCR shows increased expression of SNAI2 in KO mice

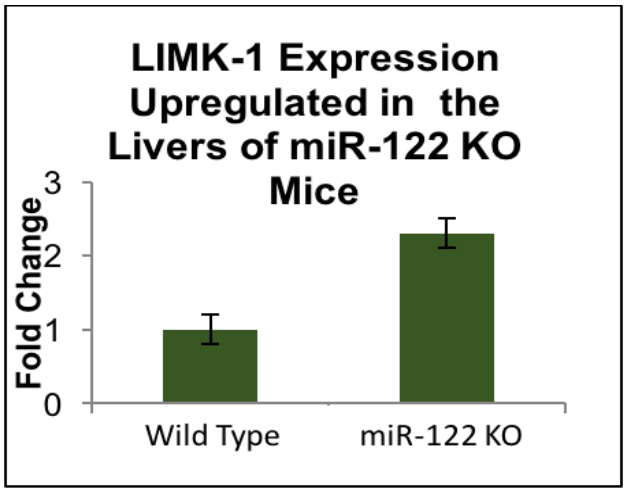

Figure 10: Real-time PCR shows increased expression of LIMK1 in KO mice

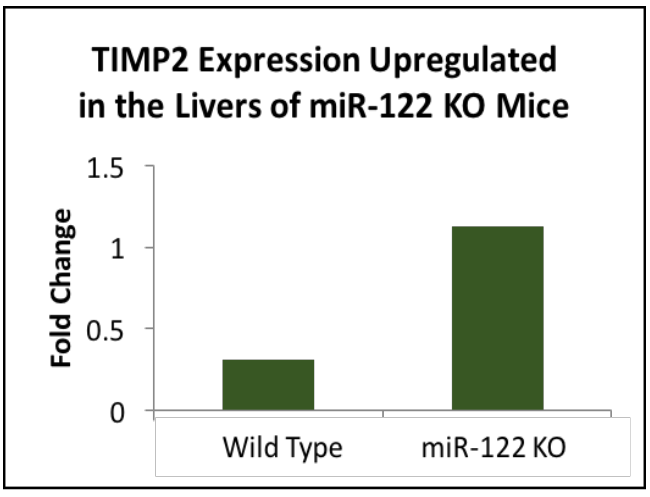

Figure 11: Real-time PCR shows increased expression of TIMP2 in KO mice

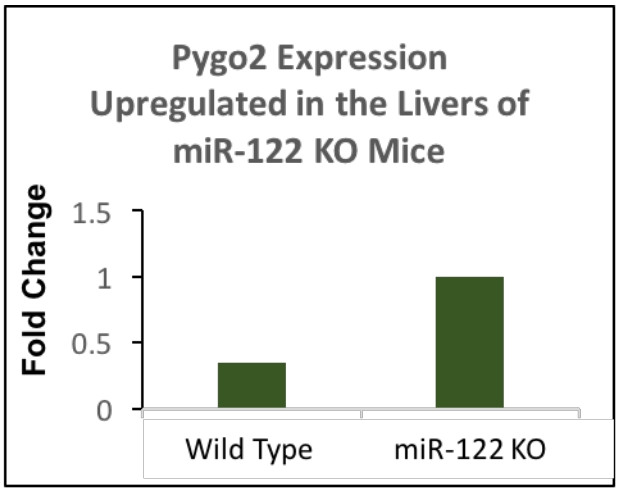

Figure 12 : Real-time PCR shows increase expression of Pygo2 in KO mice

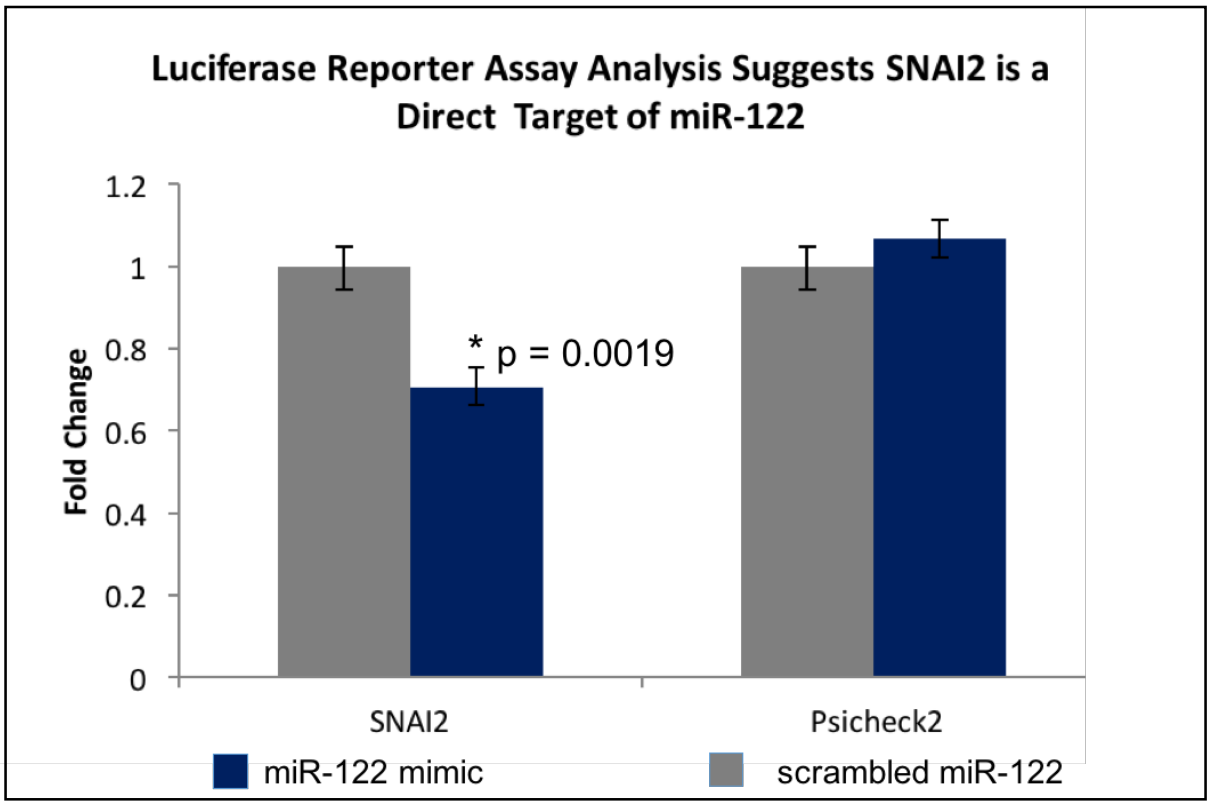

Figure 13: Luciferase Reporter Assay analysis indicates statistically significant upregulation of SNAI2 in miR-122 KO mice, suggesting direct regulation of SNAI2 by miR-122.

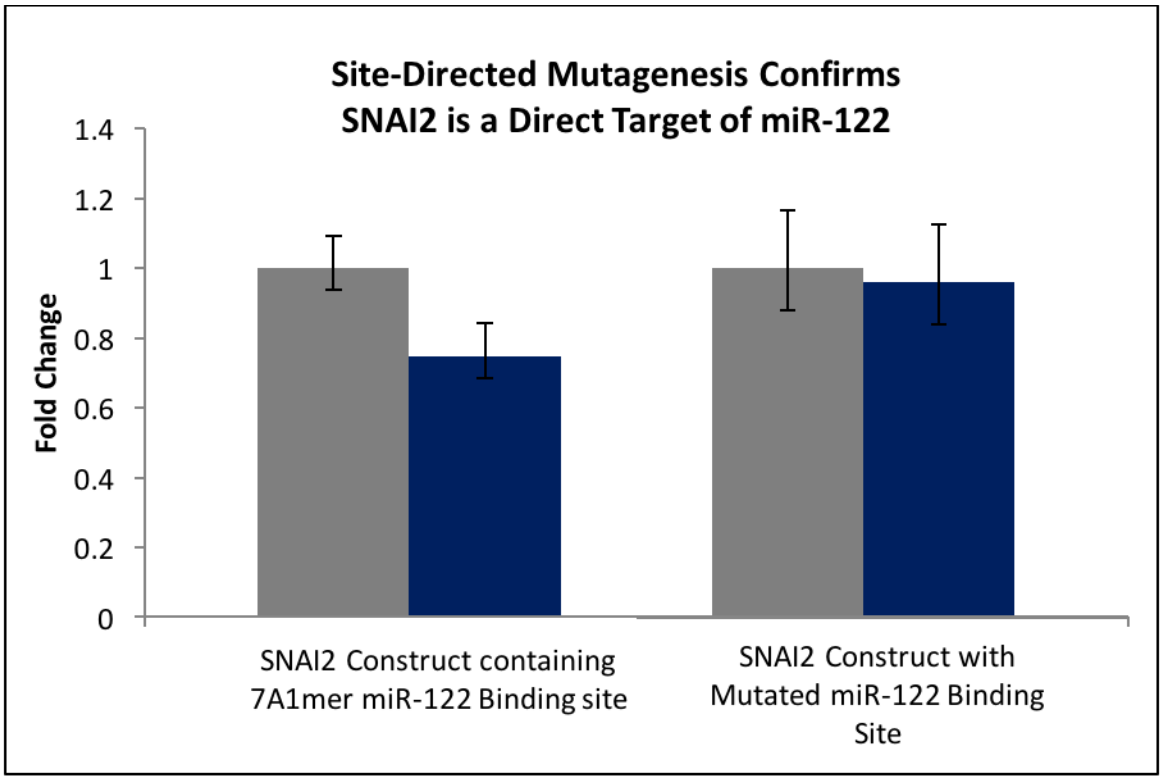

Figure 14: Mutation of the SNAI2 mirR-122 binding site downregulation of SNAI2, confirming SNAI2 as a target of miR-122
resulted in no

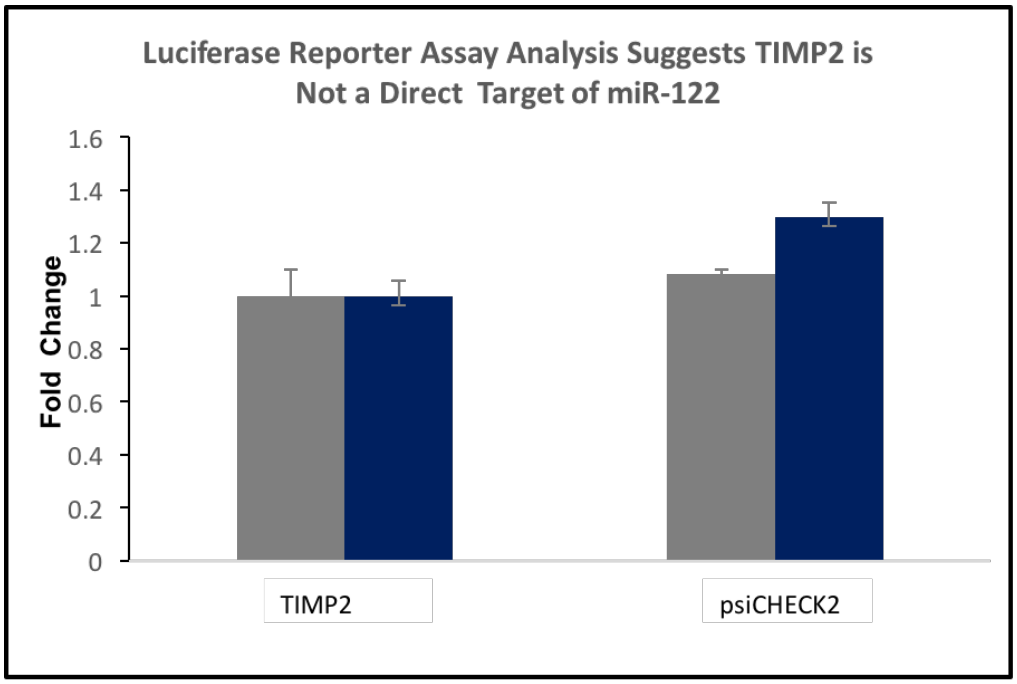

Figure 15: Luciferase Reporter Assay analysis did not indicate statistically significant upregulation of TIMP2 in miR-122 KO mice, suggesting direct regulation of SNAI2 by miR-122.

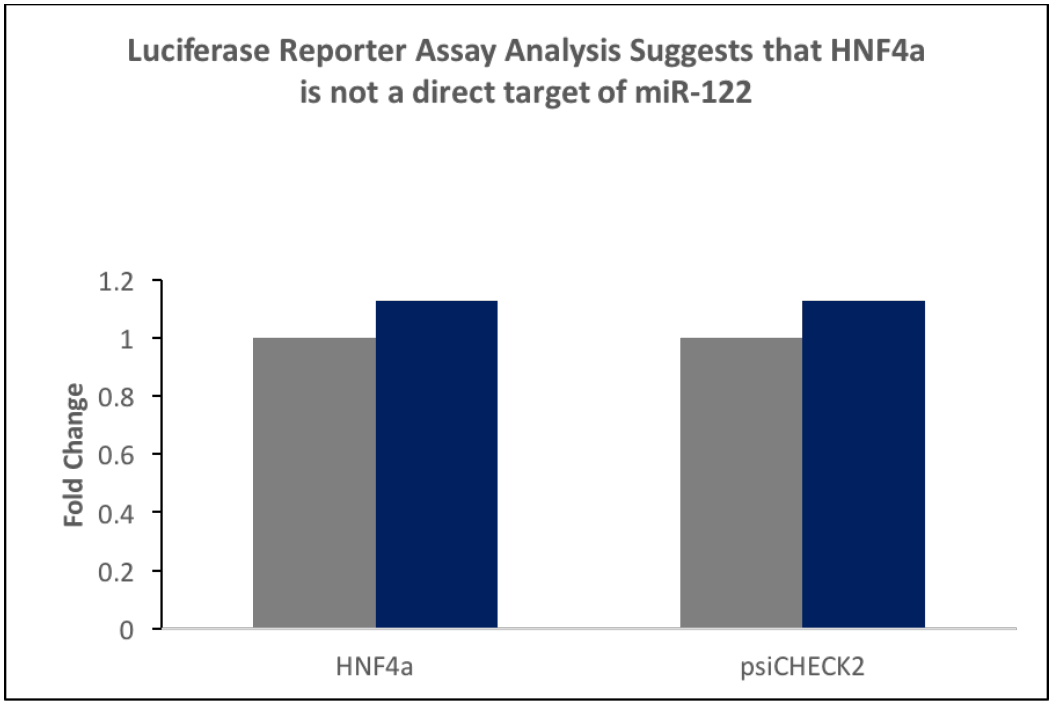

Figure 16: Luciferase Reporter Assay analysis did not indicate statistically significant upregulation of HNF4a in miR-122 KO mice, suggesting direct regulation of SNAI2 by miR-122.

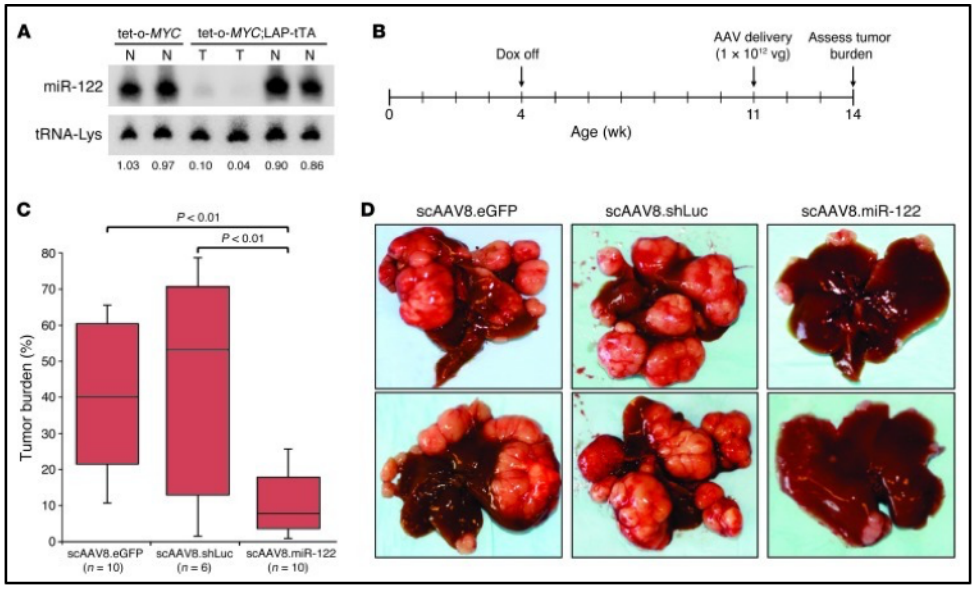

Figure 17: AAV-mediated delivery of miR-122 impedes liver tumor growth in tet-o-MYC;LAP-tTA mice.
(A) Northern blot showing miR-122 expression in normal liver (N) or tumor (T) from mice of the indicated genotypes. The normalized miR-122 level is presented below each lane. (B) Time line of miR-122 delivery experiment. Dox, doxycycline; vg, vector genomes. (C) Gross tumor burden of livers from control-treated and miR-122–treated animals, as determined by quantification of tumor area using the ImageJ software package (http://rsbweb.nih.gov/ij/). Each box represents the range of tumor burden observed. The ends of the boxes represent the 25th and 75th percentiles, the bars indicate the 10th and 90th percentiles, and horizontal lines within the boxes represent the median. (D) Representative images of livers from control-treated or miR-122–treated animals.

Shu-Hao et a, J Clin Invest. 2012 Aug 1; 122(8): 2871–2883.

VI. Sponsorship & Acknowledgements

Sponsorship

2014 Second-year Transformational Experience Program Award

Acknowledgements

Kalpana Ghoshal, PhD
The Ohio State University
College of Medicine, Department of Pathology

Samson Jacob, PhD
The Ohio State University
Department of Molecular Virology, Immunology & Medical Genetics

Huban Kutay, PhD
Department of Pathology

Kun-yu Teng
Department of Molecular, Cellular, and Developmental Biology

Juan Barajas
Department of Pathology

Works Cited

1. Szabo G, Bala S. MicroRNAs in liver disease. *Nature reviews Gastroenterology & hepatology*. 2013;10(9):542-552. doi:10.1038/nrgastro.2013.87.

2. Hsu S, Wang B, Kota J, et al. Essential metabolic, anti-inflammatory, and anti-tumorigenic functions of miR-122 in liver. *The Journal of Clinical Investigation*. 2012;122(8):2871-2883. doi:10.1172/JCI63539.

3. Thakral S, Ghoshal K. miR-122 is a Unique Molecule with Great Potential in Diagnosis, Prognosis of Liver Disease, and Therapy Both as miRNA Mimic and Antimir. *Current gene therapy*. 2015;15(2):142-150.

4. Hsu S, Wang B, Kutay H, et al. Hepatic Loss of miR-122 Predisposes Mice to Hepatobiliary Cyst and Hepatocellular Carcinoma upon Diethylnitrosamine Exposure. *The American Journal of Pathology*. 2013;183(6):1719-1730. doi:10.1016/j.ajpath.2013.08.004.

5. Altekruse SF, McGlynn KA, Reichman ME. Hepatocellular carcinoma incidence, mortality, and survival trends in the United States from 1975 to 2005. *J Clin Oncol.* 2009;27(9):1485–1491. doi: 10.1200/JCO.2008.20.7753.

6. Filipowicz W, Grosshans H. The liver-specific microRNA miR-122: biology and therapeutic potential. Prog Drug Res. 2011;67:221–238.

7. Bai S, Nasser MW, Wang B, et al. MicroRNA-122 Inhibits Tumorigenic Properties of Hepatocellular Carcinoma Cells and Sensitizes These Cells to Sorafenib. *The Journal of Biological Chemistry*. 2009;284(46):32015-32027. doi:10.1074/jbc.M109.016774.

8. Yang PC, Shih J. Thre EMT regulator slug and lung carcinogenesis. Carcinogenesis. 2011.0(0): 1-6doi:10.1093/carcin/bgr110
9. C.C. Alves, F. Carneiro, H. Hoefler, K.F. Becker. Role of the epithelial–mesenchymal transition regulator Slug in primary human cancers. Front. Biosci. (Landmark Ed.), 14 (2009), pp. 3035–3050
10. Côme C, Arnoux V, Bibeau F, Savagner P. Roles of the transcription factors snail and slug during mammary morphogenesis and breast carcinoma progression. *Journal of Mammary Gland Biology and Neoplasia*. 2004;9(2):183-193. doi:10.1023/B:JOMG.0000037161.91969.de.

11. Kumar, Brijesh, Mallikarjunachari V.n. Uppuladinne, Vinod Jani, Uddhavesh Sonavane, Rajendra R. Joshi, and Sharmila A. Bapat. "Auto-regulation of Slug Mediates Its Activity during Epithelial to Mesenchymal Transition." *Biochimica Et Biophysica Acta (BBA) - Gene Regulatory Mechanisms* 1849.9 (2015): 1209-218. Web.

12. Kai, Alan Ka-Lun, Lo Kong Chan, Regina Cheuk-Lam Lo, Joyce Man-Fong Lee, Carmen Chak-Lui Wong, Jack Chun-Ming Wong, and Irene Oi-Lin Ng. "Downregulation of TIMP2 via HIF-1α/miR-210/HIF-3α Regulatory Feedback Circuit Enhances Cancer Metastasis in Hepatocellular Carcinoma." *Hepatology* (2016):

13. Bo, S., Jian, S., Ying, Z., Fang, L., Hong, X., Yan-hua, M., Zhi-gang, Z., Shuo, Z., Bang-min, Y., You-Hua, W., Xi, Z., Xiao- Hong, A., Hui, L., Hao, J., & Qi, S. (2016). Diallyl disulfide suppresses epithelial-mesenchymal transition, invasion and proliferation by downregulation of LIMK1 in gastric cancer. *Oncotarget, 7*(9), 10498-10512.

14. A.K. Cheng, E.J. Robertson. The murine *LIM kinase* gene (*LIMK*) encodes a novel serine threonine kinase expressed predominantly in trophoblast giant cells and the developing nervous system, Mech Dev, 52 (1995), pp. 187–197

15. Mardilovich, K., Baugh, M., Crighton, D., Kowalczyk, D., Gabrielsen, M., Munro, J., Croft, D., Lourenco, F., James, D., Kalna, G., McGarry, L., Rath, O., Shanks, E., Garnett, M., McDermott, U., Brookfield, J., Charles, M., Hammonds, T., & Olson, M. (2015). LIM kinase inhibitors disrupt mitotic microtubule organization and impair tumor cell proliferation. *Oncotarget, 6*(36), 38469-38486.

16. Suravajhala, Prashanth, and Tiratha Raj Singh. "Is HNF4A a Candidate to Study Zinc Finger Protein Slug?" *International Journal of Bioinformatics Research and Applications IJBRA* 11.4 (2015): 366.

17. Zhang B, Wang J, Wang X, et al. Proteogenomic characterization of human colon and rectal cancer. *Nature*. 2014;513(7518):382-387. doi:10.1038/nature13438.

18. Zhou C, Zhang Y, Dai J, et al. Pygo2 functions as a prognostic factor for glioma due to its up-regulation of H3K4me3 and promotion of MLL1/MLL2 complex recruitment. *Scientific Reports*. 2016;6:22066. doi:10.1038/srep22066.

19. Darnell RB. HITS-CLIP: panoramic views of protein-RNA regulation in living cells. *Wiley interdisciplinary reviews RNA*. 2010;1(2):266-286. doi:10.1002/wrna.31.

20. Moore, Michael J., Chaolin Zhang, Emily Conn Gantman, Aldo Mele, Jennifer C. Darnell, and Robert B. Darnell. "Mapping Argonaute and Conventional RNA-binding Protein Interactions with RNA at Single-nucleotide Resolution Using HITS-CLIP and CIMS Analysis." *Nat Protoc Nature Protocols* 9.2 (2014): 263-93.

21. Bourboulia D, Stetler-Stevenson WG. Matrix MetalloProteinases (MMPs) andTissue Inhibitors of MetalloProteinases (TIMPs): positive and negative regulators intumor cell adhesion. *Seminars in cancer biology*. 2010;20(3):161-168. doi:10.1016/j.semcancer.2010.05.002.

22. Julia Winter, Stephanie Jung, Sarina Keller, Richard I. Gregory & Sven Diederichs. *Nature Cell Biology* 11, 228 - 234 (2009). doi:10.1038/ncb0309-228